Infrared spectroscopy and equilibrium structure of $H_2O^+(X\#\ ^2B_1)$

T. R. Huet, C. J. Pursell, W. C. Ho, B. M. Dinelli, and T. Oka

Citation: The Journal of Chemical Physics **97**, 5977 (1992); doi: 10.1063/1.463735
View online: http://dx.doi.org/10.1063/1.463735
View Table of Contents: http://aip.scitation.org/toc/jcp/97/9
Published by the American Institute of Physics

Infrared spectroscopy and equilibrium structure of $H_2O^+(\tilde{X}\ ^2B_1)$

T. R. Huet,[a] C. J. Pursell,[b] W. C. Ho,[c] B. M. Dinelli,[d] and T. Oka
The Department of Chemistry and The Department of Astronomy and Astrophysics, The University of Chicago, Chicago, Illinois 60637

(Received 20 May 1992; accepted 16 July 1992)

A color center laser spectrometer along with velocity modulation detection was used to record the absorption spectrum of H_2O^+ produced in an AC glow discharge between 3180 and 3390 cm^{-1} with a gas mixture of He/H_2O. The predominant role of the reaction of metastable helium with H_2O has been observed. The H_2O^+ ion is also present in the spectra recorded between 3100 and 3600 cm^{-1} with a gas mixture of $He/H_2/O_2$ and some features are illustrated. The ν_1 and $\nu_2+\nu_3-\nu_2$ bands have been assigned and the previous analysis of the ν_3 band [J. Mol. Spectrosc. **127**, 1 (1988)] has been extended. The ν_1 and ν_3 states have been fitted together taking into account the vibration–rotation interaction. The molecular constants have been obtained for the ν_1 and $\nu_2+\nu_3$ states and they have been improved in the case of the ν_3 and the ground vibrational states. The equilibrium structure has been derived [$r_e=0.9992(6)$ Å, $\theta_e=109.30(10)°$] and the quadratic and cubic force field constants have been evaluated.

I. INTRODUCTION

The first information concerning the H_2O^+ cation was provided at low resolution by photoelectron spectroscopic studies.[1–4] These were followed by the high-resolution study of the electronic transition $\tilde{A}\ ^2A_1$–$\tilde{X}\ ^2B_1$, observed in emission by Lew and Heiber[5] in the visible range (3500–6800 Å). The detailed analysis of the spectrum by Lew[6] provided accurate rovibrational molecular constants for the ground vibrational state and the bending states $v_2=1,2$ of the ground electronic state $\tilde{X}\ ^2B_1$, and its structure: $r_0=0.9988$ Å and $\theta_0=110.46°$. The fact that the $\tilde{X}\ ^2B_1$ and $\tilde{A}\ ^2A_1$ states result from a Renner–Teller effect in the $^2\Pi_u$ linear state motivated a theoretical study of H_2O^+ by Jungen, Hallin, and Merer.[7] The emission system of H_2O^+ is also of interest in the study of collision processes[8,9] and Penning ionization.[10] The visible system of H_2O^+ has also been observed in absorption very recently by Das and Farley.[11]

The work of Lew and Heiber[5] was found to be of considerable interest in astrophysics. It resulted in the identification of visible emission lines from H_2O^+ in Comet Kohoutek, first by Herzberg and Lew[12] and more conclusively by Wehinger *et al.*[13] Subsequently, H_2O^+ has been identified in the same visible range in different comets: Bradfield,[14] Bennet,[15] Tuttle,[16] Giacobini–Zinner,[17] and Halley.[18]

In the past few years, the absorption spectrum of the ground electronic state of H_2O^+ has been reported in the far-infrared (FIR) and IR regions. In the FIR region, Strahan, Mueller, and Saykally[19] studied the hyperfine structure of the rotational spectrum using the laser magnetic resonance technique and a few pure rotational transitions were observed by Liu, Ho, and Oka[20] using a diode laser spectrometer. In the IR region, the ν_3 band has been characterized by Dinelli, Crofton, and Oka,[21] using a difference frequency laser spectrometer. About 70 transitions were assigned, leading to the determination of molecular constants for both the ground and the ν_3 levels. They also noticed an interaction between the ν_3 and ν_1 states and predicted the band origin of the ν_1 band. Unfortunately, this band was not observed directly because of its low intensity, but the prediction is in agreement with the most recent high-resolution photoelectron spectroscopic studies.[22,23] Using a diode laser spectrometer, the bending mode has been reinvestigated in the infrared region by Brown, Davies, and Stickland.[24] They observed 85 lines of the ν_2 band and 20 lines of the hot band $2\nu_2-\nu_2$ in the region of 1270–1750 cm^{-1}.

Among the several *ab initio* computations made for H_2O^+,[25–30] the potential calculated by Weiss *et al.*[30] for the $\tilde{X}\ ^2B_1$ state is accurate enough to reproduce the observed rovibrational transition energies within a few cm^{-1}, with the discrepancies being mainly vibrational.

In this paper, we report the direct observation of the ν_1 and $\nu_2+\nu_3-\nu_2$ bands of H_2O^+ $(\tilde{X}\ ^2B_1)$. The chemistry used to optimize the intensity of H_2O^+ lines over the stronger H_3O^+ lines, also present in the spectra, allowed us to extend the previous analysis of the ν_3 band.[21] With this observation, molecular constants in all singly excited vibrational states ν_1, ν_2, and ν_3 become available, allowing us to determine an accurate equilibrium structure of H_2O^+ and to calculate the quadratic and the cubic force field constants.

[a]Senior Research Assistant with the Fonds National de la Recherche Scientifique, Belgium.
[b]Present address: Department of Chemistry, Indiana University, Bloomington, IN 47405.
[c]Present address: Department of Physics, University of British Columbia, Vancouver, British Columbia, Canada V6T 2A6.
[d]Present address: Istituto di Spettroscopia Molecolare, Via de'Castagnoli 1, 40126 Bologna, Italy.

 0021-9606/92/215977-11$006.00

II. EXPERIMENTAL DETAILS AND RESULTS

A color center laser spectrometer was employed to record spectra of H_2O^+ in the region between 3180 and 3390 cm^{-1}. Infrared radiation was obtained by using a krypton-ion laser to pump an F_A (II)-type RbCl:Li crystal of a color center laser. The experimental setup has already been described by Ho, Pursell, and Oka.[31]

The ions were generated in a water-cooled ac glow discharge powered by a Plasmaloc RS-8 at 25 KHz. The typical voltage and current were 10 kV and 300 mA. The detection of the ions was done using the velocity modulation technique[32] and the noise substraction was done using counterpropagating beams.[33] Spectra were calibrated using H_2O (Ref. 34) and NH_3 (Ref. 35) as references. The uncertainty of the line position is estimated to be around 0.010 cm^{-1}.

The optimum gas mixture was He/H_2O at a total pressure of around 10 Torr with a few mTorr of H_2O which was basically present as an impurity in the He tank. H_2O^+ lines were also present in the spectra recorded in the range between 3100 and 3600 cm^{-1} with a chemistry optimized for the production of H_3O^+, i.e., 100 mTorr H_2, 100 mTorr O_2, and 10 Torr He.[31] Those spectra have also been considered during our analysis.

In order to fully understand the plasma chemistry, the neutral species produced in the discharge should be probed and all the neutral–neutral and ion–molecule reactions should be considered. However, by taking into account a few ion–molecule reactions, we have good insight in how to reach, in our discharge, the optimum conditions for the observation of H_2O^+. We summarize hereafter our observations for a He/H_2O discharge and, in particular, we illustrate qualitatively the main differences from that in a $He/H_2/O_2$ discharge. In the former mixture, the chemistry is particularly simple and ionization of H_2O by He^+ and metastable He* is considered. These processes have been studied by Mauclaire, Derai, and Marx[36] and by Sanders and Muschlitz,[37] respectively. The reactions of He^+ and He* ($2\,^1S, 2\,^3S$) with H_2O have been observed to have the following branching ratios for the primary ions:[36,37]

$$\begin{aligned} He^+ + H_2O \rightarrow H_2O^+ \quad & (17\%) \\ OH^+ \quad & (83\%), \end{aligned} \tag{1}$$

$$\begin{aligned} He^* + H_2O \rightarrow H_2O^+ \quad & (78.0\%) \\ OH^+ \quad & (17.8\%) \\ H^+ \quad & (3.1\%) \\ HeH^+ \quad & (0.7\%) \\ HeO^+ \quad & (0.2\%). \end{aligned} \tag{2}$$

The two main resultant ionic species are OH^+ and H_2O^+. The branching ratio producing these two ions changes drastically in reactions (1) and (2). Our observed results give good insight to the relative importance of these two processes in the production of primary ions in a glow discharge. In the spectra recorded in a He/H_2O discharge, we identified the ions OH^+, H_2O^+, H_3O^+, and HeH^+. We derived their relative concentration in the discharge from the relative intensities of the rovibrational lines. The intensity ratios $I(H_2O^+)/I(H_3O^+)$ and $I(H_2O^+)/I(OH^+)$ in the He/H_2O discharge are respectively illustrated in the Figs. 1(a) and 2(a). We estimated the relative concentration of these four ions to be around $n(HeH^+)/n(OH^+)/n(H_3O^+)/n(H_2O^+) = 1/2/20/100$. The concentration of H_3O^+ is far from negligible. Sanders and Muschlitz[37] have observed that when the pressure of H_2O increases from 0.1 to 1.0 mTorr, OH^+ is being removed and H_3O^+ is produced. This is due to the secondary reactions of H_2O^+ and OH^+ with H_2O:[38]

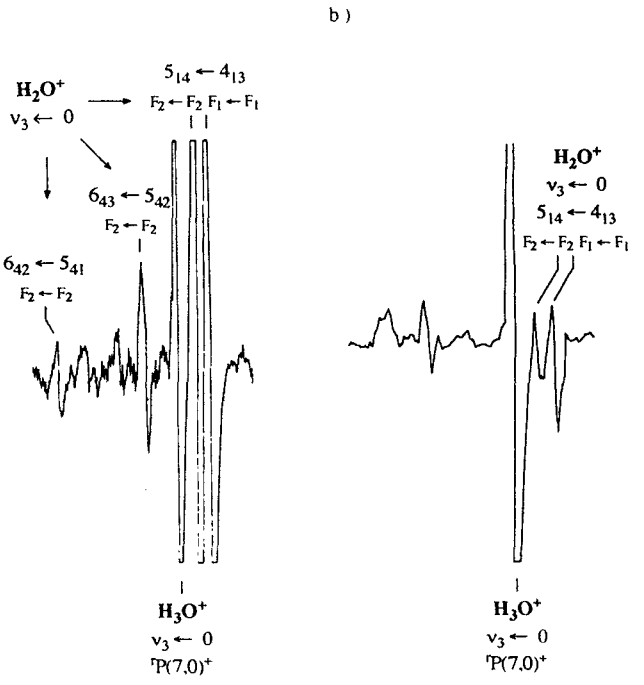

FIG. 1. Example of spectra recorded in the region of 3364 cm^{-1} by using two different chemistries: (a) 10 Torr He with H_2O as an impurity and (b) 10 Torr He with H_2O as an impurity, 100 mTorr H_2 and 100 mTorr O_2. The assignments for H_2O^+ refer to Table III and this for H_3O^+, to Ref. 31. Some lines remain unassigned.

$$H_2O^+ + H_2O \rightarrow H_3O^+ + OH, \quad k = 2.05 \times 10^{-9}\ cm^3\ s^{-1}, \tag{3}$$

$$\begin{aligned} OH^+ + H_2O \rightarrow H_2O^+ + OH, \quad & k = 1.56 \times 10^{-9}\ cm^3\ s^{-1}, \\ H_3O^+ + O, \quad & k = 1.27 \times 10^{-9}\ cm^3\ s^{-1}. \end{aligned} \tag{4}$$

Our observation confirms that the secondary reactions occur even at this low concentration of H_2O. However, a difference of 1 order of magnitude remains between the concentration of OH^+ and H_2O^+ if we take into account that more OH^+ is consumed than H_2O^+ in the final balance of the reactions (3) and (4). This suggests that the main process which is responsible for the production of the primary ions in our He/H_2O discharge is the reaction of metastable He with H_2O. Also, the fact that the observed ratio $n(HeH^+)/n(H_2O^+)$ agrees with reactions (2) gives additional support to this process.

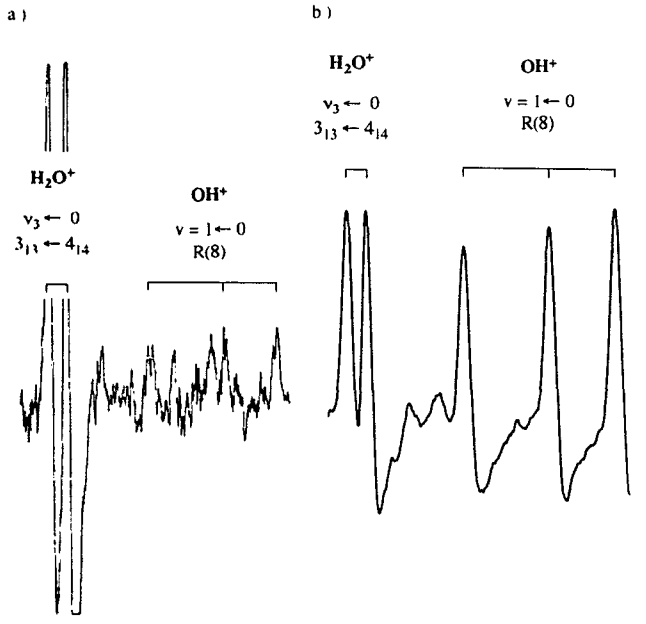

FIG. 2. Example of spectra recorded in the region of 3181 cm^{-1} by using two different chemistries: (a) 10 Torr He with H_2O as an impurity and (b) 4 Torr He with H_2O as an impurity, 80 mTorr H_2 and 80 mTorr O_2. The assignments for H_2O^+ refer to Table III and this for OH^+, to Ref. 39.

As mentioned above, H_2O^+ lines were also observed in the spectra recorded in a $He/H_2/O_2$ discharge. The chemistry of a $He/H_2/O_2$ discharge has been discussed in detail in Ref. 39 for the production of the OH^+ ion. The primary process starts from the production of O^+ by the dissociative ionization of O_2. The O^+ ions which are produced react with H_2 and a chain of hydrogen abstraction reactions takes place,[40]

$$\begin{aligned} &O^+ + H_2 \rightarrow OH^+ + H, \qquad k = 1.20\times10^{-9}\ cm^3\ s^{-1}, \\ &OH^+ + H_2 \rightarrow H_2O^+ + H, \qquad k = 1.01\times10^{-9}\ cm^3\ s^{-1}, \\ &H_2O^+ + H_2 \rightarrow H_3O^+ + H, \qquad k = 8.30\times10^{-10}\ cm^3\ s^{-1}. \end{aligned} \tag{5}$$

Figure 1(b) illustrates the relative intensity of the H_2O^+ and H_3O^+ signals when the chemistry is optimized for the observation of the H_3O^+ ion, i.e., 10 Torr He, 100 mTorr H_2, and 100 mTorr O_2.[31] In particular, we can observe a significant decrease of the H_2O^+ signals compared to the corresponding ones produced by using the He/H_2O chemistry discussed above. The chemistry that was used in Ref. 39 to optimize the signal of OH^+, 10 Torr of He, 60 mTorr of H_2, and 60 mTorr of O_2, is not very different from the chemistry used for the study of H_3O^+. The simultaneous presence of OH^+ and H_2O^+ signals of reasonable intensities has already been reported in the past.[21,39] It is illustrated in Fig. 2(b). If we compare the spectra presented in Figs. 2(a) and 2(b), the main feature is the important change in the intensity of the OH^+ signal vs the H_2O^+ signal, as in Fig. 1 for the H_3O^+ and H_2O^+ signals.

III. ANALYSIS

A. Theoretical model

The theoretical model used by Amano, Bernath, and McKellar[41] for the analysis of the ν_1 and ν_3 bands of the radical NH_2 has been applied for the isoelectronic ion H_2O^+. It was used earlier for the analysis of the ν_3 band by Dinelli, Crofton, and Oka[21] and is only briefly summarized here.

In its $^2B_1$ ground electronic state, the H_2O^+ ion has the structure of an asymmetric top with $\kappa = -0.62$. The rotation is described by the quantum numbers N, K_a, K_c. Each rotational level associated with $K_a > 0$ splits into two K_c sublevels ($K_c = N - K_a$ and $K_c = N + 1 - K_a$). In addition, the coupling between the rotational motion and the electronic spin ($S = 1/2$) splits each sublevel into two components F_1 ($J = N + S$) and F_2 ($J = N - S$). Due to the nuclear spin of the hydrogen atom ($I = 1/2$), the rovibrational levels are weighted according to the Pauli principle. It gives rise to the observation of an intensity alternation of the lines in a ratio 3:1, associated with $K_a'' + K_c''$ even and odd, respectively, when the vibrational eigenfunction of the lower level is totally symmetric.

For the ground vibrational state, the rotational structure can be described by a Hamiltonian which is a combination of the A-form reduced asymmetric rotor Hamiltonian H_{rot} of Watson[42] and the A-form reduced spin–rotation Hamiltonian H_{SR} of Brown and Sears,[43]

$$\begin{aligned} H_{rot} = {} & AN_a^2 + BN_b^2 + CN_c^2 - \Delta_N \mathbf{N}^4 - \Delta_{NK}\mathbf{N}^2 N_a^2 - \Delta_K N_a^4 \\ & - \tfrac{1}{2}[\delta_N \mathbf{N}^2 + \delta_K N_a^2, N_+^2 + N_-^2]_+ + H_N \mathbf{N}^6 \\ & + H_{NK}\mathbf{N}^4 N_a^2 + H_{KN}\mathbf{N}^2 N_a^4 + H_K N_a^6 + \cdots, \end{aligned} \tag{6}$$

$$\begin{aligned} H_{SR} = {} & \epsilon_{aa} N_a S_a + \epsilon_{bb} N_b S_b + \epsilon_{cc} N_c S_c + \Delta_N^S \mathbf{N}^2 (\mathbf{N}\cdot\mathbf{S}) \\ & + \tfrac{1}{2}\Delta_{NK}^S [\mathbf{N}^2, N_a S_a]_+ + \Delta_{KN}^S N_a^2 (\mathbf{N}\cdot\mathbf{S})^2 \\ & + \Delta_K^S N_a^3 S_a + \cdots . \end{aligned} \tag{7}$$

The c-type interaction between the ν_1 and ν_3 states gives rise to an additional term H_c,[41]

$$H_c = i\xi_{13}^c N_c + Z(N_a N_b + N_b N_a), \tag{8}$$

where ξ is related to the Coriolis coupling constant ζ by

$$\xi_{13}^c = \zeta_{13}^c C(\sqrt{\nu_1/\nu_3} + \sqrt{\nu_3/\nu_1}), \tag{9}$$

and Z is the second-order distortion constant introduced by Tanaka and Morino.[44] Because no major dependence on the quantum number ν_2 is expected, the same constants ξ and Z are involved in the similar interaction between the $\nu_2 + \nu_3$ and $\nu_1 + \nu_2$ states.

The interactions of the ν_1 and ν_3 states with $2\nu_2$ and of the $\nu_1 + \nu_2$ and $\nu_2 + \nu_3$ states with $3\nu_2$ were not included, since evidence of these perturbations was not noted during our analysis.

B. Observed spectrum

Examples of transitions assigned to the ν_1, ν_3 and $\nu_2 + \nu_3 - \nu_2$ bands are shown in Figs. 3 and 4. The splitting of

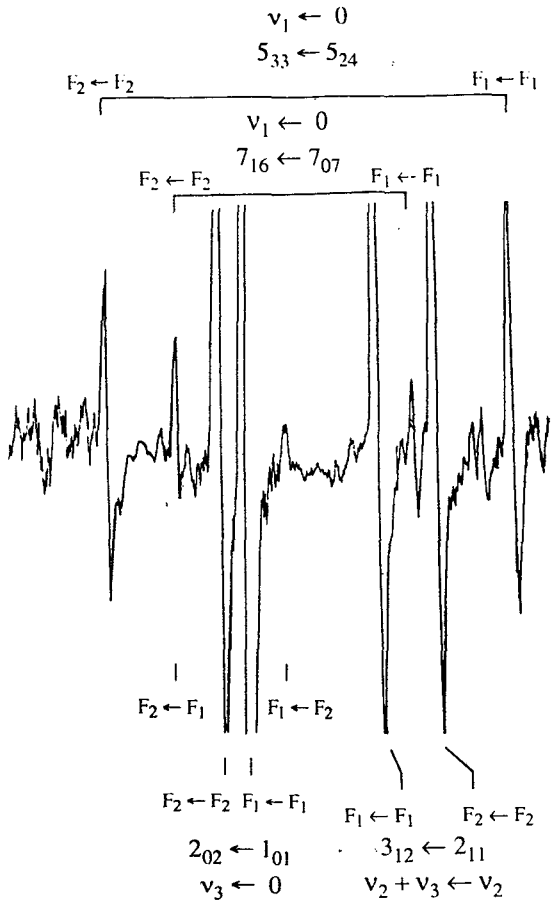

FIG. 3. Observed transitions in the region of 3299 cm^{-1} for the ν_1, ν_3, and $\nu_2+\nu_3-\nu_2$ bands of $H_2O^+(\tilde{X}\,^2B_1)$. The assignments are indicated with the label $N_{K_aK_c}$.

the lines due to the spin–rotation interaction is illustrated in Fig. 3. The most intense components give rise to a doublet structure associated with the selection rules $F_1 \leftarrow F_1$ and $F_2 \leftarrow F_2$. At low N values, weak lines $F_2 \leftarrow F_1$ and $F_1 \leftarrow F_2$ are also observed, as for instance the $2_{02} \leftarrow 1_{01}$ transition of the ν_3 band. The asymmetry splitting of the molecule in its ground electronic state is very large at low K_a values but becomes of the same order of magnitude as the spin–rotation splitting for high K_a values. This is shown in Fig. 4 for the $Q(5,4)$ lines of the ν_3 band. The intensity ratio 3:1 due to statistical weighting is also nicely illustrated.

It was observed that the ν_3 band transitions are stronger than those of the ν_1 band by approximately a factor of 4. Our observation is in agreement with the induced dipole moments theoretically calculated by Weiss *et al.*,[30] $\mu^2(\nu_1 - 0) = 0.0135$ D^2 and $\mu^2(\nu_3 - 0) = 0.0515$ D^2. The transitions of the $\nu_2+\nu_3-\nu_2$ hot band are weaker than those of the corresponding fundamental band by a factor of 5. Taking into account the fact that the induced dipole moment calculated for the hot band by Weiss *et al.*[30] does not differ significantly from the value obtained for the ν_3 band, we estimate the vibrational temperature in the discharge cell to be around 1200 K for the bending mode.

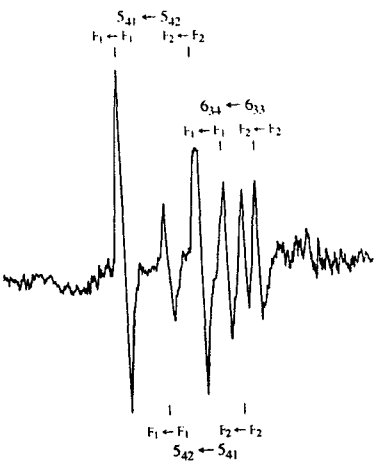

FIG. 4. Observed transitions in the region of the Q branch of the ν_3 fundamental band of $H_2O^+(\tilde{X}\,^2B_1)$. The assignments are indicated with the label $N_{K_aK_c}$.

C. Ground state

The fact that the ν_3 band is a parallel-type transition prevents an independent determination of both the upper and lower constants associated with the K_a quantum number. Also, because the upper rovibrational levels of the ν_1 perpendicular band interact with those of the ν_3 state, the ground-state molecular parameters were determined by using combination differences. A total of 57 and 189 ground-state combination differences from the ν_1 and ν_3 bands, respectively, were fitted together with the 251 combination differences obtained earlier by Lew.[6] The data were weighted according to the precision of the measurements, 0.010 cm^{-1} for the infrared data and 0.050 cm^{-1} for Lew's visible data. The standard deviation of the infrared data is 0.008 cm^{-1}, close to the measurement accuracy. The global standard deviation of the fit, including Lew's data, was 0.020 cm^{-1}. The resulting parameters are listed in Table I. They mainly characterize the $N_{K_aK_c}$ levels up to $N=8$ and $K_a=4$. A few combination differences with $K_a=5$ were only involved in parallel-type transitions and did not play a significant role in the fit. The value of the constant H_{KN} was not significant [$H_{KN} = -0.16(34)\ 10^{-5}$ cm^{-1}] and did not improve the standard deviation of the fit. It was therefore fixed at zero in the final fit. It has not been possible to separate Δ_{NK}^S from Δ_{KN}^S and to determine a significant value of Δ_N^S. Both Δ_N^S and Δ_{NK}^S values were consequently fixed at zero. We also compare in Table I our values of the molecular parameters with the results of earlier work. Our values are very consistent with those of Lew[6] and Dinelli, Crofton, and Oka[21] up to the quartic centrifugal distortion constants. The most significant difference with the results of Brown, Davies, and Stickland[24] and Strahan, Mueller, and Saykally[19] concerns the value of the B constant. Considering the more complete set of ground-state levels characterized by Lew's and our data, especially for $K_a > 2$, it seems to us that our analysis probably better reflects the

TABLE I. Molecular parameters (in cm^{-1}) for the ground vibrational level of H_2O^+ in the $\tilde{X}\,^2B_1$ state (error limits are one standard deviation and refer to the last digit).

Constant	This work	Dinelli *et al.* [21]	Lew [6]	Brown *et al.* [24]	Strahan *et al.* [19]
A	29.0359(21)	29.0370(27)	29.0256(26)	29.0366(37)	29.038365(14)
B	12.42298(58)	12.4230(24)	12.4224(14)	12.4170(15)	12.41605(10)
C	8.46921(58)	8.4691(16)	8.4693(14)	8.4684(13)	8.47208(1)
$\Delta_N\ 10^3$	1.015(13)	1.063(14)	1.00(2)	0.937(50)	0.8669(2)
$\Delta_{NK}\ 10^3$	-5.007(71)	-5.07(6)	-4.73(10)	-5.63(19)	-5.044(4)
$\Delta_K\ 10^3$	44.20(63)	43.75(60)	41.87(18)	45.72(73)	44.984(7)
$\delta_N\ 10^3$	0.3817(24)	0.3805(41)	0.370(1)	0.312(10)	0.3708(3)
$\delta_K\ 10^3$	1.795(50)	1.91(10)	1.97(19)	1.60(12)	1.947[a]
$H_N\ 10^6$	0.33(14)	1.34(22)	-	1.89(60)	-
$H_{NK}\ 10^6$	-5.1(11)	-14.3(17)	-	-9.7(29)	-
$H_{KN}\ 10^6$	-	40(8)	-	52(21)	83.2(4)
$H_K\ 10^6$	151(44)	70(31)	-	203(27)	259.5(7)
ε_{aa}	-1.0882(43)	-1.0828(51)	-1.092(18)	-1.1049(72)	-1.090(8)
ε_{bb}	-0.1130(19)	-0.1161(22)	-0.120(8)	-0.1237(37)	-0.11454(2)
ε_{cc}	0.0032(19)	0.00282(5)	-0.004(8)	-0.0061(25)	0.001685(19)
$\Delta^S_{KN}\ 10^3$	-0.72(23)	-	-	-0.98(4)	0.171(3)
$\Delta^S_K\ 10^3$	6.32(71)	5.63(47)	5(1)	12.6(8)	5.584(12)

[a] d_2 = -1.5477(36) MHz (S-reduction)

distortion effects and leads to more correct values of A_0, B_0, and C_0. The r_0 structure calculated from A_0 and B_0 is

$$r_0 = 0.999 \pm 0.015 \text{ Å},$$

$$\theta_0 = 110.5 \pm 2.5°.$$

The large uncertainties are due to the significant inertial defect of the ground vibrational state ($\Delta_0 = 0.0529$ amu Å^2). The determination of the equilibrium structure will be presented in Sec. IV.

D. The ν_1 and ν_3 vibrational levels

A total of 148 lines have been assigned to the ν_1 band and the analysis of the ν_3 band by Dinelli, Crofton, and Oka[21] has been extended up to 280 lines. They are listed in Tables II and III, respectively. In the early stage of the assignment of the ν_1 band, the computed spectrum[45] calculated with the *ab initio* spectroscopic constants derived by Weiss *et al.*[30] was found to be very helpful. For both bands, the assignments were often limited to the region between 3180 and 3390 cm^{-1}, where the spectrum was taken with a chemistry optimized for the observation of H_2O^+. Both bands have been fitted together by taking into account the *c*-type interaction, as described in Sec. III. During the least-squares procedure, the constants of the ground state were fixed at the values listed in Table I. Altogether 33 molecular parameters have been determined as presented in Table IV. The values of the sextic distortion constants H_{NK} and H_K of the ν_1 level were fixed to those of the ground state. The value of the band origin of the ν_1 band has been determined to be 3212.8598(30) cm^{-1}, which agrees well with the value predicted by Dinelli, Crofton, and Oka,[21] cf. 3213.00(9) cm^{-1}. For the ν_3 level it was found, as for the ground state, that the constant H_{KN} was not significantly determined and its value was fixed at zero. Concerning the *c*-type interaction, similar studies on H_2O (Ref. 46) and NH_2 (Ref. 41) have already shown that it is not possible to separate ξ^c_{13} from Z. We thus fixed the value of ξ^c_{13} at zero. The standard deviation of the fit is 0.009 cm^{-1}, which is comparable to the measurement accuracy. Unlike the constants given in Ref. 21, where values of centrifugal constants in the excited state differ significantly from those in the ground state, the newly determined constants do not show such remarkable differences.

E. The $\nu_2+\nu_3$ vibrational level

Among the lines which remained unassigned after the analysis of the ν_1 and ν_3 bands, we found many lines with the structure of closely spaced doublets, suggesting that they belong to a parallel band. The analysis revealed that the band origin of the lines was shifted from the ν_3 band origin to the lower frequencies by 24.8 cm^{-1}. This band was consequently assigned to the $\nu_2+\nu_3-\nu_2$ hot band. A

TABLE II. Observed transitions (in cm^{-1}) for the ν_1 fundamental band of H_2O^+ in the $\tilde{X}^2B_1$ state. The observed minus calculated wave numbers are indicated between parentheses in the unit of the last digit. The assignments are labeled $(N_{K_aK_c})' \leftarrow (N_{K_aK_c})''$; F_1 or F_2 indicates $F_1 \leftarrow F_1$ or $F_2 \leftarrow F_2$, respectively. The transitions marked with an asterisk were not included in the least-squares procedure.

$6_{34}\leftarrow5_{23}$ F_1 3406.051(3)	$7_{17}\leftarrow6_{06}$ F_2 3330.664(0)	$5_{33}\leftarrow5_{24}$ F_1 3298.685(10)	$5_{14}\leftarrow5_{05}$ F_1 3266.094(8)	$2_{02}\leftarrow2_{11}$ F_2 3186.232(-1)
$5_{33}\leftarrow4_{22}$ F_2 3393.876(7)	$7_{17}\leftarrow6_{06}$ F_1 3330.643(6)	$4_{32}\leftarrow4_{23}$ F_2 3298.353(-11)	$2_{12}\leftarrow1_{01}$ F_2 3265.923(-3)	$0_{00}\leftarrow1_{11}$ F_1 3175.672(9)
$4_{31}\leftarrow3_{22}$ F_2 3381.588(0)	$7_{07}\leftarrow6_{16}$ F_1 3327.810(-11)	$3_{31}\leftarrow3_{22}$ F_2 3298.306(2)	$2_{12}\leftarrow1_{01}$ F_1 3265.514(2)	$4_{04}\leftarrow4_{13}$ F_1 3164.291(-6)
$4_{31}\leftarrow3_{22}$ F_1 3380.794(0)	$7_{07}\leftarrow6_{16}$ F_2 3327.810(-2)	$4_{32}\leftarrow4_{23}$ F_1 3297.350(8)	$2_{20}\leftarrow2_{11}$ F_2 3260.614(-15)	$2_{12}\leftarrow3_{03}$ F_1 3164.243(-1)
$9_{28}\leftarrow8_{17}$ F_2 3379.136(20)*	$8_{27}\leftarrow8_{18}$ F_2 3324.672(0)	$3_{31}\leftarrow3_{22}$ F_1 3297.006(-4)	$2_{20}\leftarrow2_{11}$ F_1 3259.479(-10)	$4_{04}\leftarrow4_{13}$ F_1 3163.929(7)
$9_{28}\leftarrow8_{17}$ F_1 3379.068(64)*	$8_{27}\leftarrow8_{18}$ F_1 3324.021(-22)	$5_{05}\leftarrow4_{14}$ F_1 3295.703(-6)	$3_{03}\leftarrow2_{12}$ F_1 3257.456(-9)	$3_{12}\leftarrow3_{21}$ F_1 3163.199(-1)
$4_{32}\leftarrow3_{21}$ F_2 3378.203(-2)	$3_{22}\leftarrow2_{11}$ F_2 3320.079(-8)	$5_{05}\leftarrow4_{14}$ F_2 3295.619(-9)	$3_{03}\leftarrow2_{12}$ F_2 3257.151(1)	$4_{13}\leftarrow4_{22}$ F_1 3162.719(-17)
$4_{22}\leftarrow3_{13}$ F_1 3365.531(-8)	$3_{22}\leftarrow2_{11}$ F_1 3319.479(-1)	$3_{30}\leftarrow3_{21}$ F_2 3295.372(13)	$3_{21}\leftarrow3_{12}$ F_2 3256.187(10)*	$4_{13}\leftarrow4_{22}$ F_2 3162.146(-6)
$7_{26}\leftarrow6_{15}$ F_2 3362.321(-1)	$6_{16}\leftarrow5_{05}$ F_2 3317.691(0)	$3_{30}\leftarrow3_{21}$ F_1 3294.046(10	$3_{21}\leftarrow3_{12}$ F_1 3255.419(7)	$2_{11}\leftarrow2_{20}$ F_1 3161.661(-2)
$7_{26}\leftarrow6_{15}$ F_1 3362.082(0)	$6_{16}\leftarrow5_{05}$ F_1 3317.648(9)	$5_{24}\leftarrow5_{15}$ F_2 3291.431(-13)	$6_{24}\leftarrow6_{15}$ F_2 3255.082(0)	$5_{14}\leftarrow5_{23}$ F_1 3158.933(-5)
$3_{31}\leftarrow2_{20}$ F_2 3360.059(-8)	$8_{17}\leftarrow8_{08}$ F_2 3316.134(10)*	$5_{24}\leftarrow5_{15}$ F_2 3290.738(10)	$6_{24}\leftarrow6_{15}$ F_1 3254.737(-5)	$6_{15}\leftarrow6_{24}$ F_1 3150.895(-13)*
$3_{31}\leftarrow2_{20}$ F_1 3359.185(-3)	$7_{26}\leftarrow7_{17}$ F_2 3312.700(13)	$4_{31}\leftarrow4_{22}$ F_2 3290.367(1)	$4_{13}\leftarrow4_{04}$ F_2 3252.986(3)	$2_{12}\leftarrow2_{21}$ F_1 3150.685(-3)
$9_{19}\leftarrow8_{08}$ F_2 3356.842(16)	$6_{06}\leftarrow5_{15}$ F_1 3312.389(-12)	$4_{31}\leftarrow4_{22}$ F_1 3289.353(2)	$4_{22}\leftarrow4_{13}$ F_2 3252.986(4)	$6_{15}\leftarrow6_{24}$ F_2 3150.587(38)*
$9_{19}\leftarrow8_{08}$ F_1 3356.842(22)	$6_{06}\leftarrow5_{15}$ F_2 3312.356(-5)	$5_{32}\leftarrow5_{23}$ F_2 3283.425(9)	$4_{13}\leftarrow4_{04}$ F_1 3252.624(-1)	$2_{12}\leftarrow2_{21}$ F_2 3149.360(6)
$9_{09}\leftarrow8_{18}$ F_2 3356.055(-10)	$7_{26}\leftarrow7_{17}$ F_1 3312.059(14)	$4_{23}\leftarrow4_{14}$ F_2 3282.888(47)*	$4_{22}\leftarrow4_{13}$ F_1 3252.418(-4)	$5_{05}\leftarrow5_{14}$ F_1 3146.756(7)
$9_{09}\leftarrow8_{18}$ F_1 3356.055(-13)	$2_{20}\leftarrow1_{11}$ F_2 3310.147(19)	$5_{32}\leftarrow5_{23}$ F_1 3282.608(3)	$5_{23}\leftarrow5_{14}$ F_2 3252.316(-6)	$5_{05}\leftarrow5_{14}$ F_2 3146.359(-4)
$6_{25}\leftarrow5_{14}$ F_2 3354.076(-7)	$2_{20}\leftarrow1_{11}$ F_1 3309.140(-12)	$6_{15}\leftarrow6_{06}$ F_2 3282.428(7)	$5_{23}\leftarrow5_{14}$ F_1 3251.896(4)	$3_{13}\leftarrow3_{22}$ F_1 3143.128(-3)
$6_{25}\leftarrow5_{14}$ F_1 3353.759(12)	$7_{35}\leftarrow7_{26}$ F_2 3306.994(14)	$4_{23}\leftarrow4_{14}$ F_1 3282.052(1)	$1_{11}\leftarrow0_{00}$ F_1 3249.199(-40)*	$2_{02}\leftarrow3_{13}$ F_1 3142.112(1)
$8_{17}\leftarrow7_{26}$ F_1 3346.279(-6)*	$7_{35}\leftarrow7_{26}$ F_1 3306.391(-22)	$6_{15}\leftarrow6_{06}$ F_1 3282.014(19)	$2_{11}\leftarrow2_{02}$ F_1 3236.508(-3)	$3_{13}\leftarrow3_{22}$ F_2 3142.112(5)
$8_{17}\leftarrow7_{26}$ F_2 3346.150(19)*	$5_{15}\leftarrow4_{04}$ F_2 3305.025(0)	$3_{13}\leftarrow2_{02}$ F_2 3279.910(0)	$2_{02}\leftarrow1_{11}$ F_1 3236.403(-6)	$2_{02}\leftarrow3_{13}$ F_2 3141.853(4)
$5_{24}\leftarrow4_{13}$ F_2 3344.783(-6)	$5_{15}\leftarrow4_{04}$ F_1 3304.955(5)	$3_{13}\leftarrow2_{02}$ F_1 3279.657(5)	$2_{11}\leftarrow2_{02}$ F_1 3236.002(-4)	$3_{13}\leftarrow4_{04}$ F_2 3141.718(3)
$5_{24}\leftarrow4_{13}$ F_1 3344.366(8)	$6_{15}\leftarrow5_{24}$ F_1 3303.594(5)	$5_{14}\leftarrow4_{23}$ F_1 3279.300(-2)	$2_{02}\leftarrow1_{11}$ F_2 3235.693(-39)*	$3_{13}\leftarrow4_{04}$ F_1 3141.581(5)
$8_{18}\leftarrow7_{07}$ F_2 3343.771(-9)	$6_{15}\leftarrow5_{24}$ F_2 3303.237(4)	$4_{04}\leftarrow3_{13}$ F_1 3277.400(-13)	$1_{10}\leftarrow1_{01}$ F_1 3232.242(0)	$3_{03}\leftarrow4_{14}$ F_1 3126.584(10)
$8_{18}\leftarrow7_{07}$ F_1 3343.771(4)	$6_{34}\leftarrow6_{25}$ F_2 3302.175(-12)	$4_{04}\leftarrow3_{13}$ F_2 3277.244(-13)	$2_{21}\leftarrow3_{12}$ F_1 3192.409(3)	$3_{03}\leftarrow4_{14}$ F_2 3126.403(-3)
$8_{08}\leftarrow7_{17}$ F_2 3342.290(-1)	$6_{25}\leftarrow6_{16}$ F_2 3301.479(-9)	$6_{33}\leftarrow6_{24}$ F_2 3275.558(28)*	$1_{01}\leftarrow1_{10}$ F_1 3192.194(-7)	$5_{15}\leftarrow5_{24}$ F_1 3120.585(-5)
$8_{08}\leftarrow7_{17}$ F_1 3342.290(-10)	$6_{34}\leftarrow6_{25}$ F_1 3301.479(-3)	$3_{22}\leftarrow3_{13}$ F_1 3274.857(10)	$2_{21}\leftarrow3_{12}$ F_1 3191.425(-1)	$4_{14}\leftarrow5_{05}$ F_2 3119.918(0)*
$3_{21}\leftarrow2_{12}$ F_2 3336.081(-2)	$6_{25}\leftarrow6_{16}$ F_1 3300.833(13)	$6_{33}\leftarrow6_{24}$ F_1 3274.857(-20)*	$1_{11}\leftarrow2_{02}$ F_2 3187.966(23)	$5_{15}\leftarrow5_{24}$ F_2 3119.878(30)
$3_{21}\leftarrow2_{12}$ F_1 3335.201(-16)	$5_{33}\leftarrow5_{24}$ F_2 3299.521(0)	$2_{21}\leftarrow2_{12}$ F_2 3272.292(-19)	$1_{11}\leftarrow2_{02}$ F_1 3187.287(10)	$4_{14}\leftarrow5_{05}$ F_1 3119.842(5)*
$4_{23}\leftarrow3_{12}$ F_2 3333.657(-22)*	$7_{16}\leftarrow7_{07}$ F_2 3299.376(-13)	$2_{21}\leftarrow2_{12}$ F_1 3271.235(2)	$2_{02}\leftarrow2_{11}$ F_1 3186.748(2)	$1_{10}\leftarrow2_{21}$ F_1 3117.426(7)
$4_{23}\leftarrow3_{12}$ F_1 3333.133(-04)*	$7_{16}\leftarrow7_{07}$ F_1 3298.889(-35)*	$5_{14}\leftarrow5_{05}$ F_2 3266.469(1)		

total of 76 lines have been assigned and are listed in Table V. The same *c*-type interaction that existed between the levels ν_1 and ν_3 was expected between the levels $\nu_1+\nu_2$ and $\nu_2+\nu_3$. Unfortunately, we were not able to observe the hot band $\nu_1+\nu_2-\nu_2$ in our spectra, probably because of its low intensity. Consequently, a procedure similar to that employed by Dinelli, Crofton, and Oka[21] to fit the ν_3 band without the ν_1 band has been used for the $\nu_2+\nu_3-\nu_2$ band. First, the constants of the lower level of the transition, ν_2, were fixed to the values obtained by Lew[6] from data characterizing this state up to $N=6$ and $K_a=3$. Next, during the least-squares procedure, we fixed the constants describing the *c*-type interaction to the values obtained previously for that between ν_1 and ν_3. Finally, we fixed all but one of the molecular parameters for $\nu_1+\nu_2$ to some estimated values. Dinelli, Crofton, and Oka[21] fixed the three principal rotation constants to fit the approximate band origin for ν_1. In our case, it was found that the value of $A(\nu_1+\nu_2)$ estimated from the value of $A(\nu_2+\nu_3)+\alpha_3^A-\alpha_1^A$ (see Sec. IV) did not allow us to reproduce correctly the interaction between the two vibrational levels $\nu_1+\nu_2$ and $\nu_2+\nu_3$. Consequently, we decided to fix the band origin of $\nu_1+\nu_2-\nu_2$ with the help of *ab initio* calculations[30] and to fit the *A* constant of the $\nu_1+\nu_2$ state. Since the vibrational band origin of the $\nu_2+\nu_3-\nu_2$ band predicted by the *ab initio* calculations is too low by around 4.5 cm^{-1}, we estimated the band origin of the $\nu_1+\nu_2-\nu_2$ band to be 3194.0 cm^{-1}. The *B* and *C* constants of $\nu_1+\nu_2$ were constrained, assuming that $\gamma_{12}^B=\gamma_{23}^B$ and $\gamma_{12}^C=\gamma_{23}^C$ (see Sec. IV). The quartic centrifugal distortion and spin–rotation constants of $\nu_1+\nu_2$ were fixed to the fitted values of the corresponding parameters of $\nu_2+\nu_3$. The 15 parameters which have been determined are listed in Table VI. The value of H_{NK} is most probably meaningless because it was not determined for the ν_2 level. However, it was found necessary to fit this constant for the upper level in order to include the transitions at *N* higher than 6 and to fit them within the standard deviation of the fit, i.e., 0.011 cm^{-1}.

IV. EQUILIBRIUM MOLECULAR STRUCTURE

In order to derive the structure of the ground electronic state of H_2O^+ at the equilibrium position, the principal rotational constants *A*, *B*, and *C* of the ground vibrational state have to be corrected by the contributions of the vibrational motion, the centrifugal distortion, and the electronic interaction.[47] The variation of the principal rotational constants, labeled $B^\mu(\mu=A,B,C)$, with the vibra-

TABLE III. Observed transitions (in cm^{-1}) for the ν_3 fundamental band of H_2O^+ in the $\tilde{X}\,^2B_1$ state. The observed minus calculated wave numbers are indicated between parentheses in the unit of the last digit. The assignments are $(N_{K_aK_c})' \leftarrow (N_{K_aK_c})''$; F_1 or F_2 indicates $F_1 \leftarrow F_1$ or $F_2 \leftarrow F_2$, respectively. The $F_1 \leftarrow F_2$ and $F_2 \leftarrow F_1$ transitions are labeled as F_{12} and F_{21}, respectively. The transitions marked with an asterisk were not included in the least-squares procedure.

$9_{37}\leftarrow8_{36}$ F_1 3422.321(-21)*	$6_{16}\leftarrow5_{15}$ F_1 3361.258(-4)	$2_{02}\leftarrow1_{01}$ F_2 3299.291(-5)	$5_{42}\leftarrow5_{41}$ F_1 3238.910(-10)	$3_{13}\leftarrow4_{14}$ F_2 3181.621(-1)
$9_{37}\leftarrow8_{36}$ F_2 3422.242(-3)*	$6_{16}\leftarrow5_{15}$ F_2 3361.241(-4)	$2_{02}\leftarrow1_{01}$ F_1 3299.242(-1)	$5_{41}\leftarrow5_{42}$ F_2 3238.843(-3)	$3_{13}\leftarrow4_{14}$ F_1 3181.590(1)
$10_{1,10}\leftarrow9_{19}$ F_1 3418.653(0)	$6_{51}\leftarrow5_{50}$ F_1 3356.702(-33)*	$2_{02}\leftarrow1_{01}$ F_{12}3299.153(-9)*	$6_{34}\leftarrow6_{33}$ F_1 3238.784(-18)	$3_{03}\leftarrow4_{04}$ F_1 3179.244(-1)
$10_{1,10}\leftarrow9_{19}$ F_2 3418.653(3)	$6_{51}\leftarrow5_{50}$ F_2 3355.963(-20)*	$2_{12}\leftarrow1_{11}$ F_{21}3295.423(-1)	$5_{42}\leftarrow5_{41}$ F_2 3238.745(0)	$3_{03}\leftarrow4_{04}$ F_2 3179.176(2)
$8_{36}\leftarrow7_{35}$ F_1 3405.911(-7)	$5_{24}\leftarrow4_{23}$ F_1 3352.827(-3)	$2_{12}\leftarrow1_{11}$ F_1 3294.935(-3)	$6_{34}\leftarrow6_{33}$ F_2 3238.719(-14)	$8_{27}\leftarrow8_{26}$ F_2 3176.217(20)*
$8_{36}\leftarrow7_{35}$ F_2 3405.778(-7)	$5_{32}\leftarrow4_{31}$ F_1 3352.787(4)	$2_{12}\leftarrow1_{11}$ F_2 3294.607(-3)	$0_{00}\leftarrow1_{01}$ F_1 3238.173(-2)	$6_{16}\leftarrow6_{15}$ F_1 3174.870(10)
$9_{09}\leftarrow8_{08}$ F_2 3405.273(0)	$5_{24}\leftarrow4_{23}$ F_2 3352.673(0)	$4_{13}\leftarrow4_{14}$ F_2 3294.261(15)	$0_{00}\leftarrow1_{01}$ F_{12}3238.093(0)	$6_{16}\leftarrow6_{15}$ F_2 3174.448(-3)
$9_{09}\leftarrow8_{08}$ F_1 3405.273(0)	$5_{32}\leftarrow4_{31}$ F_2 3352.381(4)	$4_{13}\leftarrow4_{14}$ F_1 3293.985(08)	$6_{42}\leftarrow6_{43}$ F_1 3237.296(0)	$3_{22}\leftarrow4_{23}$ F_2 3170.162(0)
$9_{19}\leftarrow8_{18}$ F_2 3404.929(-2)	$5_{33}\leftarrow4_{32}$ F_1 3351.396(0)	$3_{12}\leftarrow3_{13}$ F_2 3280.716(11)	$6_{42}\leftarrow6_{43}$ F_2 3237.148(1)	$3_{22}\leftarrow4_{23}$ F_1 3170.019(0)
$9_{19}\leftarrow8_{18}$ F_1 3404.929(-6)	$5_{33}\leftarrow4_{32}$ F_2 3351.004(3)	$3_{12}\leftarrow3_{13}$ F_1 3280.408(9)	$6_{43}\leftarrow6_{42}$ F_1 3236.800(-7)	$3_{12}\leftarrow4_{13}$ F_2 3167.378(8)
$8_{27}\leftarrow7_{26}$ F_1 3401.952(3)	$5_{05}\leftarrow4_{04}$ F_2 3348.789(-5)	$1_{01}\leftarrow0_{00}$ F_{21}3279.694(0)	$6_{43}\leftarrow6_{42}$ F_2 3236.689(29)*	$3_{12}\leftarrow4_{13}$ F_1 3167.276(-5)
$8_{27}\leftarrow7_{26}$ F_2 3401.903(0)	$5_{05}\leftarrow4_{04}$ F_1 3348.789(5)	$1_{01}\leftarrow0_{00}$ F_1 3279.608(-3)	$7_{43}\leftarrow7_{44}$ F_1 3235.693(13)	$3_{21}\leftarrow4_{22}$ F_2 3164.921(6)
$7_{34}\leftarrow6_{33}$ F_1 3395.100(-33)*	$5_{15}\leftarrow4_{14}$ F_{21}3345.960(-22)*	$2_{11}\leftarrow2_{12}$ F_2 3268.477(27)*	$7_{43}\leftarrow7_{44}$ F_2 3235.579(17)	$3_{21}\leftarrow4_{22}$ F_1 3164.792(5)
$7_{34}\leftarrow6_{33}$ F_2 3394.925(-16)*	$5_{15}\leftarrow4_{14}$ F_1 3345.654(-4)	$2_{11}\leftarrow2_{12}$ F_1 3268.110(-10)	$3_{13}\leftarrow3_{12}$ F_1 3232.661(-13)	$3_{31}\leftarrow4_{32}$ F_2 3163.772(-18)
$8_{08}\leftarrow7_{07}$ F_2 3391.459(-7)	$5_{15}\leftarrow4_{14}$ F_2 3345.625(-3)	$5_{23}\leftarrow5_{24}$ F_1 3267.876(-30)*	$5_{24}\leftarrow5_{23}$ F_1 3232.470(3)*	$3_{30}\leftarrow4_{31}$ F_2 3163.436(4)
$8_{08}\leftarrow7_{07}$ F_1 3391.459(-4)	$5_{41}\leftarrow4_{40}$ F_1 3345.310(10)	$5_{23}\leftarrow5_{24}$ F_2 3267.876(-31)*	$3_{13}\leftarrow3_{12}$ F_2 3232.430(-30)*	$3_{31}\leftarrow4_{32}$ F_1 3163.436(-11)
$8_{18}\leftarrow7_{17}$ F_1 3390.824(-6)	$5_{42}\leftarrow4_{41}$ F_1 3345.256(6)	$1_{10}\leftarrow1_{11}$ F_2 3261.669(2)	$5_{24}\leftarrow5_{23}$ F_2 3232.385(-7)*	$3_{30}\leftarrow4_{31}$ F_1 3163.083(-5)
$8_{18}\leftarrow7_{17}$ F_2 3390.824(0)	$4_{13}\leftarrow3_{12}$ F_2 3345.092(8)	$1_{10}\leftarrow1_{11}$ F_1 3261.634(3)	$5_{51}\leftarrow5_{50}$ F_1 3231.048(-5)	$4_{14}\leftarrow5_{15}$ F_1 3162.647(-13)
$7_{35}\leftarrow6_{34}$ F_1 3388.536(-19)*	$4_{13}\leftarrow3_{12}$ F_1 3345.070(6)	$4_{22}\leftarrow4_{23}$ F_1 3260.363(5)	$5_{50}\leftarrow5_{51}$ F_1 3231.048(-6)	$4_{14}\leftarrow5_{15}$ F_2 3162.647(-24)*
$7_{35}\leftarrow6_{34}$ F_2 3388.355(-12)*	$5_{41}\leftarrow4_{40}$ F_2 3344.588(4)	$4_{22}\leftarrow4_{23}$ F_2 3260.322(5)	$5_{51}\leftarrow5_{50}$ F_2 3230.799(2)	$4_{04}\leftarrow5_{05}$ F_1 3161.045(4)
$7_{26}\leftarrow6_{25}$ F_1 3386.454(20)	$5_{42}\leftarrow4_{41}$ F_2 3344.536(1)	$2_{20}\leftarrow2_{21}$ F_{21}3256.499(4)	$5_{50}\leftarrow5_{51}$ F_2 3230.799(1)	$4_{04}\leftarrow5_{05}$ F_2 3161.006(-2)
$7_{26}\leftarrow6_{25}$ F_2 3386.388(19)	$4_{22}\leftarrow3_{21}$ F_1 3340.406(-4)	$3_{21}\leftarrow3_{22}$ F_1 3256.249(18)	$6_{52}\leftarrow6_{51}$ F_1 3229.094(-5)	$4_{23}\leftarrow5_{24}$ F_2 3148.923(4)
$7_{43}\leftarrow6_{42}$ F_1 3384.160(2)	$4_{22}\leftarrow3_{21}$ F_2 3340.144(-13)	$3_{21}\leftarrow3_{22}$ F_2 3256.157(19)	$6_{51}\leftarrow6_{52}$ F_1 3229.094(-15)	$4_{23}\leftarrow5_{24}$ F_1 3148.865(6)
$7_{43}\leftarrow6_{42}$ F_2 3383.794(7)	$4_{23}\leftarrow3_{22}$ F_{21}3335.893(-14)*	$2_{21}\leftarrow2_{20}$ F_{21}3255.211(-8)	$6_{52}\leftarrow6_{51}$ F_2 3228.883(0)	$4_{13}\leftarrow5_{14}$ F_1 3145.016(0)
$7_{44}\leftarrow6_{43}$ F_1 3383.509(0)	$4_{23}\leftarrow3_{22}$ F_1 3334.770(-3)	$2_{20}\leftarrow2_{21}$ F_1 3254.762(-9)	$6_{51}\leftarrow6_{52}$ F_2 3228.883(-9)	$4_{13}\leftarrow5_{14}$ F_2 3144.990(8)
$6_{24}\leftarrow5_{23}$ F_1 3383.352(5)	$4_{23}\leftarrow3_{22}$ F_2 3334.485(-2)	$2_{20}\leftarrow2_{21}$ F_2 3254.662(0)	$7_{52}\leftarrow7_{53}$ F_1 3226.896(16)	$5_{15}\leftarrow6_{16}$ F_1 3143.768(-1)
$6_{24}\leftarrow5_{23}$ F_2 3383.311(0)	$4_{04}\leftarrow3_{03}$ F_{21}3333.908(-18)*	$1_{11}\leftarrow1_{10}$ F_{21}3254.577(-8)	$7_{52}\leftarrow7_{53}$ F_2 3226.715(23)	$5_{15}\leftarrow6_{16}$ F_2 3143.768(-1)
$7_{44}\leftarrow6_{43}$ F_2 3383.110(2)	$4_{04}\leftarrow3_{03}$ F_2 3333.734(-5)	$1_{11}\leftarrow1_{10}$ F_1 3253.818(-3)	$1_{11}\leftarrow2_{12}$ F_2 3220.083(-2)	$5_{05}\leftarrow6_{06}$ F_1 3142.834(3)
$6_{15}\leftarrow5_{14}$ F_2 3380.942(9)	$4_{04}\leftarrow3_{03}$ F_1 3333.683(-4)	$1_{11}\leftarrow1_{10}$ F_2 3253.683(0)	$6_{61}\leftarrow6_{60}$ F_1 3219.904(8)	$5_{05}\leftarrow6_{06}$ F_2 3142.806(0)
$6_{15}\leftarrow5_{14}$ F_1 3380.884(8)	$4_{31}\leftarrow3_{30}$ F_1 3332.365(8)	$2_{21}\leftarrow2_{20}$ F_1 3253.496(-2)	$6_{60}\leftarrow6_{61}$ F_1 3219.904(8)	$4_{32}\leftarrow5_{33}$ F_2 3141.193(2)
$7_{07}\leftarrow6_{06}$ F_1 3377.448(3)	$4_{32}\leftarrow3_{31}$ F_1 3331.949(3)	$2_{21}\leftarrow2_{20}$ F_2 3253.383(-2)	$1_{11}\leftarrow2_{12}$ F_1 3219.827(2)	$4_{32}\leftarrow5_{33}$ F_1 3141.032(2)
$7_{07}\leftarrow6_{06}$ F_2 3377.448(-5)	$4_{31}\leftarrow3_{30}$ F_2 3331.723(6)	$1_{11}\leftarrow1_{10}$ F_1 3252.922(3)	$6_{61}\leftarrow6_{60}$ F_1 3219.624(11)	$4_{22}\leftarrow5_{23}$ F_1 3139.997(3)*
$7_{17}\leftarrow6_{16}$ F_1 3376.298(4)	$4_{32}\leftarrow3_{31}$ F_2 3331.308(2)	$3_{22}\leftarrow3_{21}$ F_1 3250.070(-2)	$6_{60}\leftarrow6_{61}$ F_2 3219.624(11)	$4_{22}\leftarrow5_{23}$ F_2 3139.997(-38)*
$7_{17}\leftarrow6_{16}$ F_2 3376.298(14)	$4_{14}\leftarrow3_{13}$ F_{12}3329.748(-2)	$3_{22}\leftarrow3_{21}$ F_2 3249.997(-5)	$1_{01}\leftarrow2_{02}$ F_1 3217.650(1)	$4_{31}\leftarrow5_{32}$ F_1 3139.851(2)
$7_{52}\leftarrow6_{51}$ F_1 3375.595(-9)*	$4_{14}\leftarrow3_{13}$ F_1 3329.400(-6)	$3_{30}\leftarrow3_{31}$ F_1 3248.443(15)	$1_{01}\leftarrow2_{02}$ F_2 3217.596(1)	$4_{41}\leftarrow5_{42}$ F_1 3134.312(-5)
$7_{53}\leftarrow6_{52}$ F_1 3375.595(9)*	$4_{14}\leftarrow3_{13}$ F_2 3329.343(-8)	$3_{31}\leftarrow3_{30}$ F_1 3248.307(12)	$1_{01}\leftarrow2_{02}$ F_{12}3217.512(-1)*	$5_{24}\leftarrow6_{25}$ F_2 3127.920(0)
$7_{52}\leftarrow6_{51}$ F_2 3375.053(13)*	$3_{12}\leftarrow2_{11}$ F_{21}3325.735(-3)	$3_{30}\leftarrow3_{31}$ F_2 3248.269(8)	$7_{62}\leftarrow7_{61}$ F_2 3217.388(10)*	$5_{24}\leftarrow6_{25}$ F_1 3127.900(-1)
$7_{53}\leftarrow6_{52}$ F_2 3375.053(40)*	$3_{12}\leftarrow2_{11}$ F_2 3325.088(-1)	$3_{31}\leftarrow3_{30}$ F_2 3248.138(10)	$6_{25}\leftarrow6_{24}$ F_1 3217.373(-9)	$6_{16}\leftarrow7_{17}$ F_1 3124.825(4)
$6_{33}\leftarrow5_{32}$ F_1 3373.710(0)	$3_{12}\leftarrow2_{11}$ F_1 3325.022(-10)	$4_{31}\leftarrow4_{32}$ F_1 3247.505(-3)	$6_{25}\leftarrow6_{24}$ F_2 3217.266(-14)	$6_{16}\leftarrow7_{17}$ F_2 3124.825(9)
$6_{33}\leftarrow5_{32}$ F_2 3373.430(-2)	$3_{21}\leftarrow2_{20}$ F_{21}3319.733(-2)	$4_{31}\leftarrow4_{32}$ F_2 3247.375(-5)	$4_{14}\leftarrow4_{13}$ F_1 3216.296(6)	$6_{06}\leftarrow7_{07}$ F_1 3124.329(-8)
$6_{34}\leftarrow5_{33}$ F_1 3370.348(6)	$3_{21}\leftarrow2_{20}$ F_1 3318.412(3)	$5_{32}\leftarrow5_{33}$ F_1 3247.197(-10)	$4_{14}\leftarrow4_{13}$ F_2 3216.021(5)	$6_{06}\leftarrow7_{07}$ F_2 3124.329(9)
$6_{34}\leftarrow5_{33}$ F_2 3370.068(3)	$3_{21}\leftarrow2_{20}$ F_2 3317.900(0)	$5_{32}\leftarrow5_{33}$ F_2 3247.084(-5)	$1_{10}\leftarrow2_{11}$ F_2 3212.166(-2)	$5_{14}\leftarrow6_{15}$ F_1 3123.814(-5)
$6_{25}\leftarrow5_{24}$ F_1 3370.068(5)	$3_{03}\leftarrow2_{02}$ F_{21}3317.526(20)*	$4_{32}\leftarrow4_{31}$ F_1 3246.599(-6)	$1_{10}\leftarrow2_{11}$ F_1 3211.968(1)	$5_{14}\leftarrow6_{15}$ F_2 3123.745(1)
$6_{25}\leftarrow5_{24}$ F_2 3369.963(-1)	$3_{03}\leftarrow2_{02}$ F_2 3317.375(5)	$4_{32}\leftarrow4_{31}$ F_2 3246.467(-10)	$1_{10}\leftarrow2_{11}$ F_{12}3211.322(3)	$5_{33}\leftarrow6_{34}$ F_2 3118.521(-15)
$7_{62}\leftarrow6_{61}$ F_1 3366.672(-5)	$3_{03}\leftarrow2_{02}$ F_1 3317.325(3)	$2_{12}\leftarrow2_{11}$ F_{21}3245.763(2)	$2_{12}\leftarrow3_{13}$ F_2 3200.726(-1)	$5_{33}\leftarrow6_{34}$ F_1 3118.445(-4)
$7_{62}\leftarrow6_{61}$ F_2 3365.889(-36)	$3_{22}\leftarrow2_{21}$ F_{21}3317.227(4)	$2_{12}\leftarrow2_{11}$ F_1 3245.274(0)	$2_{12}\leftarrow3_{13}$ F_1 3200.640(0)	$5_{32}\leftarrow6_{33}$ F_2 3115.763(3)
$6_{42}\leftarrow5_{41}$ F_1 3364.743(-3)	$3_{22}\leftarrow2_{21}$ F_1 3315.914(21)	$2_{12}\leftarrow2_{11}$ F_2 3245.108(-4)	$2_{02}\leftarrow3_{03}$ F_1 3197.982(5)	$5_{32}\leftarrow6_{33}$ F_1 3115.676(7)
$6_{43}\leftarrow5_{42}$ F_1 3364.524(-6)	$3_{22}\leftarrow2_{21}$ F_2 3315.394(2)	$5_{33}\leftarrow5_{32}$ F_1 3243.739(2)	$2_{02}\leftarrow3_{03}$ F_2 3197.928(2)	$5_{23}\leftarrow6_{24}$ F_1 3115.209(-16)
$6_{42}\leftarrow5_{41}$ F_2 3364.244(1)	$3_{13}\leftarrow2_{12}$ F_1 3312.476(-4)	$5_{33}\leftarrow5_{32}$ F_2 3243.651(5)	$5_{15}\leftarrow5_{14}$ F_1 3196.714(17)	$5_{23}\leftarrow6_{24}$ F_2 3115.209(-13)
$6_{43}\leftarrow5_{42}$ F_2 3364.019(-8)	$3_{13}\leftarrow2_{12}$ F_2 3312.356(-9)	$4_{23}\leftarrow4_{22}$ F_1 3243.348(18)	$5_{15}\leftarrow5_{14}$ F_2 3196.335(-28)*	$6_{25}\leftarrow7_{26}$ F_1 3107.186(-17)
$5_{14}\leftarrow4_{13}$ F_2 3363.886(3)	$5_{14}\leftarrow5_{15}$ F_2 3310.528(-9)	$4_{23}\leftarrow4_{22}$ F_2 3243.287(22)	$2_{21}\leftarrow3_{22}$ F_2 3191.622(0)	$6_{25}\leftarrow7_{26}$ F_2 3107.186(-13)
$5_{14}\leftarrow4_{13}$ F_1 3363.852(-1)	$5_{14}\leftarrow5_{15}$ F_1 3310.215(-8)	$4_{41}\leftarrow4_{40}$ F_1 3240.595(1)	$2_{21}\leftarrow3_{22}$ F_1 3191.326(5)	$7_{17}\leftarrow8_{18}$ F_1 3105.739(2)
$6_{06}\leftarrow5_{05}$ F_2 3363.256(-7)	$2_{11}\leftarrow1_{10}$ F_{21}3302.954(3)	$4_{40}\leftarrow4_{41}$ F_1 3240.595(-10)	$2_{20}\leftarrow3_{21}$ F_2 3189.259(-15)	$7_{17}\leftarrow8_{18}$ F_2 3105.739(9)
$6_{06}\leftarrow5_{05}$ F_1 3363.245(-2)	$2_{11}\leftarrow1_{10}$ F_1 3302.122(4)	$4_{41}\leftarrow4_{40}$ F_2 3240.380(4)	$2_{20}\leftarrow3_{21}$ F_1 3188.941(-10)	$7_{07}\leftarrow8_{08}$ F_1 3105.533(26)*
$5_{23}\leftarrow4_{22}$ F_1 3362.376(0)	$2_{11}\leftarrow1_{10}$ F_2 3302.044(-4)	$4_{40}\leftarrow4_{41}$ F_2 3240.380(-7)	$2_{11}\leftarrow3_{12}$ F_2 3188.542(-02)	$7_{07}\leftarrow8_{08}$ F_2 3105.511(18)*
$5_{23}\leftarrow4_{22}$ F_2 3362.248(-5)	$2_{02}\leftarrow1_{01}$ F_{21} 3299.376(-3)	$5_{41}\leftarrow5_{42}$ F_1 3239.017(-6)	$2_{11}\leftarrow3_{12}$ F_1 3188.326(11)	$6_{15}\leftarrow7_{16}$ F_2 3103.532(-18)

TABLE IV. Molecular parameters (in cm^{-1}) for the ν_1 and ν_3 vibrational levels of H_2O^+ in the $\tilde{X}\,^2B_1$ state (error limits are one standard deviation and refer to the last digit).

Constant	ν_1	ν_3	
	This work	This work	Dinelli *et al.* [21]
ν_0	3212.8598(30)	3259.0360(20)	3259.031(3)
A	28.3928(14)	27.84879(64)	27.8501(21)
B	12.19289(74)	12.26881(49)	12.286(7)
C	8.29520(74)	8.33146(49)	8.324(5)
$\Delta_N\,10^3$	0.987(11)	1.0077(65)	1.437(15)
$\Delta_{NK}\,10^3$	-4.971(32)	-5.127(40)	-6.10(16)
$\Delta_K\,10^3$	43.33(14)	40.558(53)	40.69(35)
$\delta_N\,10^3$	0.3750(43)	0.3732(28)	0.566(11)
$\delta_K\,10^3$	1.883(59)	1.641(38)	4.69(35)
$H_N\,10^6$	0.141(86)	0.301(44)	1.34[a]
$H_{NK}\,10^6$	-5.1[a]	-6.13(47)	-14.3[a]
$H_{KN}\,10^6$	-	-	40[a]
$H_K\,10^6$	151[a]	131.49(99)	70[a]
ε_{aa}	-1.0732(56)	-1.0209(17)	-1.018(6)
ε_{bb}	-0.1130(17)	-0.1111(13)	-0.113(4)
ε_{cc}	0.0027(17)	0.0024(13)	0.00286(10)
$\Delta^S_{KN}\,10^3$	-0.55(21)	-0.719(83)	-
$\Delta^S_K\,10^3$	7.37(83)	5.84(12)	5.7(7)
ξ^c_{13}	0.0[b]		0.0
Z	0.44277(50)		0.442(5)

[a] fixed to the ground vibrational state value listed in Table I.

[b] fixed at zero (see text).

tional motion is expressed by the polynomial series in the vibrational quantum numbers v_i as

$$B^\mu(v_1,v_2,v_3)=B^\mu_e-\sum_{i=1}^{3}\alpha^\mu_i(v_i+\tfrac{1}{2})+\sum_{i=1}^{3}\sum_{j\geq i=1}^{3}\gamma^\mu_{ij}(v_i+\tfrac{1}{2})\times(v_j+\tfrac{1}{2})+\cdots. \quad (10)$$

So far, the data available from this work and from the literature characterize the ground, ν_1, ν_2, ν_3, $2\nu_2$, $\nu_1+\nu_2$, and $\nu_2+\nu_3$ vibrational states. Therefore, all the γ constants could not be determined. To be consistant with the data, we decided to consider only the α corrections in the determination of the equilibrium constants. As expected for a light molecule like H_2O^+, a poor convergence of the series was observed for the rotational constant A_e compared to B_e and C_e. We consequently estimated the error on B_e and C_e at 10^{-3} cm^{-1} and on A_e at 10^{-1} cm^{-1}. The contribution of the centrifugal distortion and of the electron was found to be within the estimated error and was not considered here. The value of the equilibrium constants and of the α corrections are listed in Table VII and are compared with the *ab initio* values of Weiss *et al.*[30] The equilibrium bond length r_e and angle θ_e have been calculated from the most reliable constants, B_e and C_e. The error on r_e and θ_e is estimated from the nonzero value of the inertial defect. A very good agreement is observed with the *ab initio* results.

V. POTENTIAL CONSTANTS

The characterization of the rovibrational structure of the ground vibrational state and of the three vibrational

TABLE V. Observed transitions (in cm^{-1}) for the $\nu_2+\nu_3-\nu_2$ hot band of H_2O^+ in the $\tilde{X}\,^2B_1$ state. The observed minus calculated wave numbers are indicated between parentheses in the unit of the last digit. The assignments are labeled $(N_{K_aK_c})' \leftarrow (N_{K_aK_c})''$; F_1 or F_2 indicates $F_1 \leftarrow F_1$ or $F_2 \leftarrow F_2$, respectively. The transitions marked with an asterisk were not included in the least-squares procedure.

$9_{09} \leftarrow 8_{08}$ F_2 3379.109(-1)	$6_{06} \leftarrow 5_{05}$ F_2 3338.367(24)*	$4_{22} \leftarrow 3_{21}$ F_2 3313.450(8)	$3_{13} \leftarrow 2_{12}$ F_1 3287.004(53)*	$3_{30} \leftarrow 3_{31}$ F_1 3220.678(-6)
$9_{09} \leftarrow 8_{08}$ F_1 3379.109(-4)	$6_{06} \leftarrow 5_{05}$ F_1 3338.234(10)	$4_{04} \leftarrow 3_{03}$ F_2 3309.038(-3)	$3_{13} \leftarrow 2_{12}$ F_2 3286.751(9)	$3_{30} \leftarrow 3_{31}$ F_2 3220.391(-8)
$9_{19} \leftarrow 8_{18}$ F_1 3378.498(10)	$5_{23} \leftarrow 4_{22}$ F_1 3336.081(0)	$4_{04} \leftarrow 3_{03}$ F_1 3308.990(-5)	$2_{11} \leftarrow 1_{10}$ F_1 3277.711(4)	$0_{00} \leftarrow 1_{01}$ F_1 3213.486(1)
$9_{19} \leftarrow 8_{18}$ F_2 3378.481(-2)	$5_{23} \leftarrow 4_{22}$ F_2 3335.807(-12)	$4_{23} \leftarrow 3_{22}$ F_1 3308.402(-3)	$2_{11} \leftarrow 1_{10}$ F_2 3277.244(11)	$1_{11} \leftarrow 2_{12}$ F_2 3195.408(-2)
$8_{27} \leftarrow 7_{26}$ F_1 3376.146(7)	$6_{16} \leftarrow 5_{15}$ F_1 3335.333(-6)	$4_{23} \leftarrow 3_{22}$ F_2 3308.114(-10)	$2_{02} \leftarrow 1_{01}$ F_2 3274.429(3)	$1_{11} \leftarrow 2_{12}$ F_1 3195.024(8)
$8_{27} \leftarrow 7_{26}$ F_2 3376.028(-8)	$6_{16} \leftarrow 5_{15}$ F_2 3335.296(-7)	$4_{32} \leftarrow 3_{31}$ F_1 3304.088(9)	$2_{02} \leftarrow 1_{01}$ F_1 3274.369(2)	$1_{01} \leftarrow 2_{02}$ F_1 3193.011(0)
$8_{18} \leftarrow 7_{17}$ F_1 3364.580(-5)	$5_{24} \leftarrow 4_{23}$ F_1 3326.616(-63)*	$4_{14} \leftarrow 3_{13}$ F_1 3303.741(3)	$2_{12} \leftarrow 1_{11}$ F_1 3269.548(-3)	$1_{01} \leftarrow 2_{02}$ F_2 3192.949(-7)
$8_{18} \leftarrow 7_{17}$ F_2 3364.566(-7)	$5_{24} \leftarrow 4_{23}$ F_2 3326.462(-20)*	$4_{14} \leftarrow 3_{13}$ F_2 3303.635(2)	$2_{12} \leftarrow 1_{11}$ F_2 3268.991(-19)	$1_{10} \leftarrow 2_{11}$ F_2 3187.092(-13)
$7_{26} \leftarrow 6_{25}$ F_1 3360.582(-7)	$5_{05} \leftarrow 4_{04}$ F_2 3324.227(-18)	$4_{32} \leftarrow 3_{31}$ F_2 3303.092(3)	$1_{01} \leftarrow 0_{00}$ F_1 3254.737(-3)	$1_{10} \leftarrow 2_{11}$ F_1 3186.773(-9)
$7_{26} \leftarrow 6_{25}$ F_2 3360.466(17)	$5_{05} \leftarrow 4_{04}$ F_1 3324.021(-6)	$3_{12} \leftarrow 2_{11}$ F_1 3298.962(12)	$1_{10} \leftarrow 1_{11}$ F_1 3236.689(10)	$2_{02} \leftarrow 3_{03}$ F_1 3173.304(-14)
$7_{07} \leftarrow 6_{06}$ F_2 3352.048(16)	$5_{15} \leftarrow 4_{14}$ F_1 3319.869(5)	$3_{12} \leftarrow 2_{11}$ F_2 3298.840(12)	$1_{10} \leftarrow 1_{11}$ F_2 3236.689(5)	$2_{02} \leftarrow 3_{03}$ F_2 3173.293(26)*
$7_{07} \leftarrow 6_{06}$ F_1 3352.048(4)	$5_{15} \leftarrow 4_{14}$ F_2 3319.794(-9)	$3_{03} \leftarrow 2_{02}$ F_2 3292.602(10)	$3_{21} \leftarrow 3_{22}$ F_1 3229.854(4)	$2_{11} \leftarrow 3_{12}$ F_2 3163.831(-9)
$7_{17} \leftarrow 6_{16}$ F_1 3350.222(-1)	$4_{13} \leftarrow 3_{12}$ F_2 3318.836(-22)*	$3_{03} \leftarrow 2_{02}$ F_1 3292.535(1)	$3_{21} \leftarrow 3_{22}$ F_2 3229.737(21)*	$2_{11} \leftarrow 3_{12}$ F_1 3163.772(-9)
$7_{17} \leftarrow 6_{16}$ F_2 3350.196(-6)	$4_{13} \leftarrow 3_{12}$ F_1 3318.740(17)	$3_{21} \leftarrow 2_{20}$ F_1 3291.957(0)	$2_{21} \leftarrow 2_{20}$ F_1 3227.385(-6)	$3_{12} \leftarrow 4_{13}$ F_1 3140.921(-10)
$6_{25} \leftarrow 5_{24}$ F_1 3344.129(-15)	$4_{22} \leftarrow 3_{21}$ F_1 3313.898(6)	$3_{21} \leftarrow 2_{20}$ F_2 3291.149(17)	$2_{21} \leftarrow 2_{20}$ F_2 3227.184(0)	$3_{12} \leftarrow 4_{13}$ F_2 3140.921(-14)
$6_{25} \leftarrow 5_{24}$ F_2 3343.944(15)				

states ν_1, ν_2, and ν_3, allowed the determination of the quadratic and the cubic force field constants. We used the experimental values of the band origins of the fundamental transitions determined from the analysis instead of the equilibrium vibrational frequencies. For a light molecule like H_2O^+, this approximation is somewhat crude but still

TABLE VI. Molecular parameters (in cm^{-1}) for the $\nu_2+\nu_3$ vibrational level of H_2O^+ in the $\tilde{X}\,^2B_1$ state (error limits are one standard deviation and refer to the last digit).

Constant	$\nu_2+\nu_3$	$\nu_1+\nu_2$
ν_0	3234.2469(47)	3194.0[a]
A	31.7911(30)	32.084(18)
B	12.3354(20)	12.25[a]
C	8.1820(20)	8.14[a]
$\Delta_N\ 10^3$	1.175(26)	1.175[a]
$\Delta_{NK}\ 10^3$	-8.50(21)	-8.50[a]
$\Delta_K\ 10^3$	74.32(28)	74.32[a]
$\delta_N\ 10^3$	0.309(12)	0.309[a]
$\delta_K\ 10^3$	5.76(29)	5.76[a]
$H_N\ 10^6$	-	-
$H_{NK}\ 10^6$	-27.6(49)	-27.6[a]
$H_{KN}\ 10^6$	-	-
$H_K\ 10^6$	-	-
ε_{aa}	-1.5111(98)	-1.5111[a]
ε_{bb}	-0.1233(29)	-0.1233[a]
ε_{cc}	0.0097(29)	0.0097[a]
$\Delta^S_{KN}\ 10^3$	-	-
$\Delta^S_K\ 10^3$	15.0(13)	15.0[a]
ξ^c_{13}	0.0[a]	
Z	0.44277[a]	

[a] fixed value (see text).

TABLE VII. Equilibrium rotational constants, associated vibrational corrections and structure of H_2O^+ in the $\tilde{X}\,^2B_1$ state.

a) Equilibrium Rotational constants (in cm^{-1})

	Experimental[1]	Theoretical[2]
A_e	27.789	27.956
B_e	12.588	12.597
C_e	8.700	8.684
Δ (amuÅ^2)	$-8\ 10^{-3}$	$-3\ 10^{-6}$

b) Vibrational Corrections to the Equilibrium Rotational Constants (in cm^{-1})

	Experimental[1]	Theoretical[2]
α_1^A	0.6431	0.6137
α_2^A	-4.3242	-3.3436
α_3^A	1.1817	1.1089
α_1^B	0.2301	0.2435
α_2^B	-0.0535	-0.0573
α_3^B	0.1542	0.1604
α_1^C	0.1740	0.1755
α_2^C	0.1504	0.1512
α_3^C	0.1378	0.1429

c) Equilibrium Molecular Structure

	Experimental[1]	Theoretical[2]
r_e (Å)	0.9992(6)	1.0004
α_e (deg)	109.30(10)	109.0745

[1] This work and Ref. 6 (see text).
[2] Ref. 30.

TABLE VIII. Quadratic and cubic force constants in the $\tilde{X}^2B_1$ state of H_2O^+.

a) Quadratic Constants (in mdyn $Å^{-1}$)

	This work	Ref. 30[a]
f_r	5.847(16)	6.500
$f_{rr'}$	0.0344(1)	0.030
$f_{r\alpha}$	0.329(33)	0.152
f_α	0.5809(83)	0.605

b) Cubic Constants (in cm^{-1})

	This work	Ref. 30[b]
k_{111}	- 261.3	- 278.9
k_{112}	15.0	10.8
k_{222}	- 79.3	- 55.3
k_{122}	99.3	87.2
k_{133}	- 736.5	- 791.8
k_{233}	113.5	78.6

(a) With (in cm^{-1}) : $\omega_1^e = 3380.6$; $\omega_2^e = 1476.6$; $\omega_3^e = 3436.3$.

(b) See text.

gives reasonably good results. The experimental determination of the quadratic force field constants was performed by using the usual GF method developed by Wilson, Decius, and Cross[48] and the relations existing between these force constants and the quartic centrifugal distortion constants of the ground vibrational state.[47,49] The quadratic force constants f_r, $f_{rr'}$, $f_{r\alpha}$, and f_α associated with the internal coordinates have been determined by a least-squares procedure. They are listed in Table VIII together with the *ab initio* constants of Weiss *et al.*[30] The cubic potential constants have been determined by using the relationships developed by Nielsen[50] between the rovibrational constants α introduced in Eq. (10) and the quadratic and cubic potential constants associated with the dimensionless normal coordinates. To be consistent in our approach, we considered the α constants determined from the fundamental bands and neglected the γ constants. The cubic constants $k_{ss's''}$ that we have obtained are also listed in Table VIII, together with those derived by using the spectroscopic constants calculated by Weiss *et al.*[30]

VI. CONCLUSION

We have reported the analysis of the ν_1 and $\nu_2+\nu_3-\nu_2$ bands and the extension of the previous analysis of the ν_3 band[21] of H_2O^+. Around 500 lines have been assigned; these assignments could be of astrophysical interest, especially in the study of comets. The present characterization of the ν_1 vibrational state completes the previous characterization of the ν_2 and ν_3 states, and allowed us to determine the equilibrium structure and to estimate the quadratic and cubic force constants of this molecule in the ground electronic state.

This extended characterization was made possible in part because experimental conditions have been found to favor the formation of the H_2O^+ ion in our ac glow discharge over the OH^+ and H_3O^+ ions, also present in our spectra. We observed that a pure helium discharge, owing to a small water impurity in the helium tank, enhanced the H_2O^+ signals compared to the spectra recorded with a gas mixture of $He/H_2/O_2$. Some observations in our discharge have been illustrated and discussed in this paper. In the case of a gas mixture of He/H_2O, optimized for the observation of the H_2O^+ ion in the infrared region, we have observed that the reaction of metastable helium with H_2O is the dominant reaction for the production of the primary ions and that secondary reactions occur efficiently.

ACKNOWLEDGMENTS

The authors are indebted to Dr. P. Rosmus, who kindly provided a computed spectrum of rovibrational transitions calculated by using the results presented in Ref. 30. Thérèse Huet gratefully acknowledges the partial support of a NATO research fellowship from Belgium for the academic year 1990–1991. This work was supported by the NSF, Grant No. PHY 90-22647.

[1] C. R. Brundle and D. W. Turner, Proc. R. Soc. London, Ser. A **307**, 27 (1968).
[2] A. W. Potts and W. C. Price, Proc. R. Soc. London, Ser. A **326**, 181 (1972).
[3] L. Karlsson, L. Mattsson, R. Jadrny, R. G. Albridge, S. Pinchas, T. Bergmarck, and K. Siegbahn, J. Chem. Phys. **62**, 4745 (1975).
[4] R. N. Dixon, G. Duxbury, J. W. Rabelais, and L. Asbrink, Mol. Phys. **31**, 423 (1976).
[5] H. Lew and I. Heiber, J. Chem. Phys. **58**, 1246 (1973).
[6] H. Lew, Can. J. Phys. **54**, 2028 (1976).
[7] C. Jungen, K.-E. Hallin, and A. J. Merer, Mol. Phys. **40**, 25 (1980); **40**, 65 (1980).
[8] H. H. Harris and J. J. Leventhal, J. Chem. Phys. **64**, 3185 (1976).
[9] B. Friedrich, G. Niedner, M. Noll, and P. Toennies, J. Chem. Phys. **87**, 1447 (1987); **87**, 5256 (1987).
[10] M. Tsuji, J. P. Maier, H. Obase, and Y. Nishimura, Chem. Phys. Lett. **47**, 619 (1988).
[11] B. Das and J. W. Farley, J. Chem. Phys. **95**, 8809 (1991).
[12] G. Herzberg and H. Lew, Astron. Astrophys. **31**, 123 (1974).
[13] P. A. Wehinger, S. Wickoff, G. H. Herbig, G. Herzberg, and H. Lew, Astrophys. J. **190**, L43 (1974).
[14] P. Wehinger and S. Wyckoff, Astrophys. J. **192**, L41 (1974); S. Wyckoff and P. A. Wehinger, *ibid.* **204**, 604 (1976).
[15] A. H. Delsemme and M. R. Combi, Astrophys. J. **209**, L153 (1976); **228**, 330 (1979).
[16] W.-H. Ip, U. Fink, and J. R. Johnson, Astrophys. J. **293**, 609 (1985).
[17] N. Meyer-Vernet, M. A. Strauss, J. L. Steinberg, H. Spinrad, and P. J. McCarthy, Astron. J. **93**, 474 (1987).
[18] M. A. Disanti, U. Fink, and A. B. Schultz, Icarus **86**, 152 (1990).
[19] S. E. Strahan, R. P. Mueller, and R. J. Saykally, J. Chem. Phys. **85**, 1252 (1986).
[20] D.-J. Liu, W.-C. Ho, and T. Oka, J. Chem. Phys. **87**, 2442 (1987).
[21] B. M. Dinelli, M. W. Crofton, and T. Oka, J. Mol. Spectrosc. **127**, 1 (1988).

[22] J. E. Reutt, L. S. Wang, Y. T. Lee, and D. A. Shirley, J. Chem. Phys. **85**, 6928 (1986).
[23] R. G. Tonkyn, R. Wiedmann, E. R. Grant, and M. G. White, J. Chem. Phys. **95**, 7033 (1991).
[24] P. R. Brown, P. B. Davies, and R. J. Stickland, J. Chem. Phys. **91**, 3384 (1989).
[25] J. C. Leclerc, J. A. Horsley, and J. C. Lorquet, Chem. Phys. **4**, 337 (1974); A. J. Lorquet and J. C. Lorquet, *ibid.* **4**, 353 (1974).
[26] J. A. Smith, P. Jorgensen, and Y. Ohm, J. Chem. Phys. **62**, 1285 (1975).
[27] P. J. Fortune, B. J. Rosenberg, and A. C. Wahl, J. Chem. Phys. **65**, 2201 (1976).
[28] C. J. Jackels, J. Chem. Phys. **72**, 4873 (1980).
[29] A. Degli Espoti, D. G. Lister, P. Palmieri, and C. Degli Espoti, J. Chem. Phys. **87**, 6772 (1987).
[30] B. Weiss, S. Carter, P. Rosmus, H.-J. Werner, and P. J. Knowles, J. Chem. Phys. **91**, 2818 (1989).
[31] W. C. Ho, C. J. Pursell, and T. Oka, J. Mol. Spectrosc. **149**, 530 (1991).
[32] C. S. Gudeman, M. H. Begemann, J. Pfaff, and R. J. Saykally, Phys. Rev. Lett. **50**, 727 (1983).
[33] M. G. Bawendi, B. D. Rehfuss, and T. Oka, J. Chem. Phys. **93**, 6200 (1990).
[34] J. M. Flaud, C. Camy-Peyret, and R. A. Toth, in *International Tables of Selected Constants* (Pergamon, New York, 1981), Vol. 19.
[35] J. W. C. Johns (private communication).
[36] G. Mauclaire, R. Derai, and R. Marx, Int. J. Mass Spectrom. Ion Phys. **26**, 489 (1978).
[37] R. A. Sanders and E. E. Muschlitz, Int. J. Mass Spectrom. Ion Phys. **23**, 99 (1977).
[38] W. T. Huntress and R. F. Pinizzotto, J. Chem. Phys. **59**, 4742 (1973).
[39] B. D. Rehfuss, M.-F. Jagod, L.-W. Xu, and T. Oka, J. Mol. Spectrosc. **151**, 59 (1991).
[40] V. G. Anicich and W. T. Huntress, Astrophys. J. Suppl. Ser. **62**, 553 (1986).
[41] T. Amano, P. F. Bernath, and A. R. W. McKellar, J. Mol. Spectrosc. **94**, 100 (1982).
[42] J. K. G. Watson, in *Vibrational Spectra and Structure*, edited by J. R. Durig (Decker, New York, 1977), Vol. 6, pp. 1–89.
[43] J. M. Brown and T. J. Sears, J. Mol. Spectrosc. **75**, 111 (1979).
[44] T. Tanaka and Y. Morino, J. Mol. Spectrosc. **33**, 538 (1970).
[45] P. Rosmus (private communication).
[46] J. M. Flaud and C. Camy-Peyret, J. Mol. Spectrosc. **51**, 142 (1974).
[47] T. Oka and Y. Morino, J. Mol. Spectrosc. **8**, 300 (1962).
[48] E. B. Wilson, Jr., J. C. Decius, and P. C. Cross, *Molecular Vibration* (McGraw-Hill, New York, 1955).
[49] D. Kivelson, J. Chem. Phys. **22**, 904 (1954).
[50] H. H. Nielsen, Rev. Mod. Phys. **23**, 90 (1951).